Liquid Crystals
Publication details, including instructions for authors and subscription information:
http://www.informaworld.com/smpp/title~content=t713926090

Theory of the temperature-concentration phase diagrams of lyotropic liquid crystals

P. Tolédano; C. E. I. Carneiro; A. M. Figueiredo Neto

Online publication date: 06 August 2010

To cite this Article Tolédano, P. , Carneiro, C. E. I. and Neto, A. M. Figueiredo(2001) 'Theory of the temperature-concentration phase diagrams of lyotropic liquid crystals', Liquid Crystals, 28: 10, 1547 — 1551
To link to this Article: DOI: 10.1080/02678290110068956
URL: http://dx.doi.org/10.1080/02678290110068956

LIQUID CRYSTALS, 2001, VOL. 28, NO. 10, 1547–1551

Theory of the temperature–concentration phase diagrams of lyotropic liquid crystals

P. TOLÉDANO†‡, C. E. I. CARNEIRO† and A. M. FIGUEIREDO NETO†*
†Instituto de Física, Universidade de São Paulo, Caixa Postal 66318, 05315-970 São Paulo, SP, Brasil
‡Groupe Structure des Matériaux Sous Conditions Extrêmes, SNBL/ESRF, P.O. Box 220, 38043 Grenoble, France

(*Received 23 February 2001; accepted 16 May 2001*)

A phenomenological approach to the description of temperature–concentration phase diagrams in lyotropic liquid crystals is proposed. It is based on the coupling of the power expansions associated with the concentration variable, and the symmetry-breaking order parameters. Illustrative, working and real, examples of phase diagrams found in lyotropic systems are discussed.

1. Introduction

Lyotropic liquid crystals contain at least two components, one of which is a solvent and the other is formed by surfactant molecules having a hydrophilic head group and hydrophobic alkyl chain tail(s) [1]. The mixing of the two components may induce the spontaneous formation of structures showing high degrees of positional and orientational order, which are accessed by changing the concentration of surfactant and the temperature. The temperature–concentration phase diagram of a two-component surfactant–solvent system has generally a multi-eutectic topology [2], each phase displaying an optimal concentration and well-defined peaks in the phase diagram. A typical phase diagram contains isotropic (molecular, micellar or bicontinuous) phases, as well as anisotropic phases, e.g. with a lamellar, cubic, hexagonal, etc… or nematic ordering, and eventually the corresponding reversed phases, which are formed by inverted micellar aggregates [1, 2]. Two adjacent phases are in most cases separated by a two-phase region of coexistence, i.e. by first order transitions [1]. There are a few exceptions, such as the uniaxial and biaxial nematic or cholesteric phases which are separated by second order transition lines [3].

Theoretical approaches to lyotropic liquid crystal systems have focused on specific regions of their phase diagrams in which the phases can be related by a unifying structural mechanism [4–6]. But there has been, to our knowledge, no attempt to describe theoretically the variety of topologies found for the temperature–concentration phase diagrams of lyotropic mixtures, in a comprehensive way. This is due, on the one hand, to the complexity of the phase diagrams, but also to the intrinsic difficulty of taking into account simultaneously the effects of the temperature and concentration variables, which give rise to transformation mechanisms of different natures: (1) symmetry breaking transitions which are often of the reconstructive [7, 8] type; (2) concentration driven transformations [9] which result in phase separation, without symmetry change.

* Author for correspondence; e-mail: afigueiredo@if.usp.br

2. Theory

The aim of this paper is to show, in the case of a two-component lyotropic system, that an overall description of the corresponding temperature–concentration phase diagrams can be performed in the framework of a generalized Landau-type approach, in which the free energy of the system is expressed in functions of a variational concentration parameter and of the symmetry-breaking order parameter(s). Let us introduce the basic ingredients of our model through working examples of temperature–concentration phase diagrams of lyotropics. We consider first a lyotropic mixture formed by a solvent (W) and a surfactant (S), involving only isotropic molecular and micellar solutions, denoted respectively (W, S) and (W + S). We take as the concentration variable the dimensionless quantity $\rho = x_S - x_W$, where $x_S = [S]/[S] + [W]$ and $x_W = 1 - x_S$, the brackets [] designating the molar fraction. The free energy density of the mixture can be written as $\Phi(\Delta\mu, T) = F_G(\rho, T) - \Delta\mu\rho$, where $F_G(\rho, T)$ is the Helmholtz free energy per mole and $\Delta\mu$ is the chemical potential conjugated to $N\rho$, where N is the total number of moles in the system. The equilibrium line separating two

Liquid Crystals ISSN 0267-8292 print/ISSN 1366-5855 online © 2001 Taylor & Francis Ltd
http://www.tandf.co.uk/journals
DOI: 10.1080/02678290110068956

different lyotropic phases, denoted 1 and 2, is obtained analytically by the common tangent construction method proposed by Gibbs [10], which consists in expressing simultaneously the equality of the chemical potentials ($\Delta\mu_1 = \Delta\mu_2$) and the effective free energies [$\Phi(\Delta\mu_1, T) = \Phi(\Delta\mu_2, T)$]. This yields the equations:

$$\left(\frac{\partial F_G}{\partial \rho}\right)_1 = \left(\frac{\partial F_G}{\partial \rho}\right)_2 \tag{1}$$

and

$$F_G(\rho_1) - \rho_1\left(\frac{\partial F_G}{\partial \rho}\right)_1 = F_G(\rho_2) - \rho_2\left(\frac{\partial F_G}{\partial \rho}\right)_2 \tag{2}$$

where ρ_1 and ρ_2 refer to the respective concentrations in phases 1 and 2. Solving equations (1) and (2) at constant chemical potential for each temperature and concentration requires explicit knowledge of the form of $F_G(\rho, T)$. In contrast to the standard form used for F_G, which is expressed in terms of the free enthalpy for each component and of the entropy of mixing, we shall assume that $F_G(\rho, T)$ can be written as a power expansion of ρ, of degree P:

$$F_G(\rho, T) = \frac{(T - T_o)}{2}\rho^2 + \sum_{n=3}^{P} \frac{a_n}{n}\rho^n \tag{3}$$

where the a_n are constant phenomenological coefficients, and T_o is the temperature corresponding to $\rho = 0$ on the equilibrium line between phases 1 and 2. Figures 1 (*a*), 1 (*b*) and 1 (*c*) represent three among the phase diagrams obtained by solving equations (1) and (2) using specific forms of $F_G(\rho, T)$. Thus, the phase diagram of figure 1 (*a*) is obtained for $P = 4$, $a_3 < 0$ and $a_4 > 0$. It represents the equilibrium line between the molecular and micellar isotropic phases, which has a maximum at the critical point C determined by the condition $\partial^3 F_G/\partial\rho^3 = 0$. For low and high concentrations, the line is bounded by the direct and reversed critical micellar concentrations (CMC and CMC′), the direct and reversed micellar regions forming a continuum. A different situation occurs in the phase diagram shown in figure 1 (*b*) which is associated with a potential F_G expanded around the eutectic concentration ρ_E:

$$F_G(\rho - \rho_E, T) = \frac{(T - T_E)}{2}(\rho - \rho_E)^2 + \frac{a_3}{3}(\rho - \rho_E)^3 + \frac{a_4}{4}(\rho - \rho_E)^4 \tag{4}$$

where T_E is the eutectic temperature. Here, a_3 and a_4 are divalent coefficients, i.e. a_3 coincides with the two values of opposite signs taken by the slopes of $T(\rho)$ at $\rho = \rho_E$. In the same way the two values taken by a_4 are determined by the slopes of $T(\rho)$ for $\rho = \rho_{CMC}$ and $\rho = \rho_{CMC'}$. In the phase diagram of figure 1 (*b*) the direct and reversed micellar phases do not overlap, and meet at the eutectic point E, at which the solution crystallizes. More complex phase diagrams are obtained within the same approach by using higher degree expansions of $F_G(\rho, T)$. The phase diagram shown in figure 1 (*c*) corresponds to a fifth degree expansion of F_G around $\rho = \rho_E$. It contains both a critical point C (ρ_c being determined by one of the roots of the equation $\partial^3 F_G/\partial\rho^3 = 0$) and a eutectic point E. a_3 is again a divalent coefficient representing

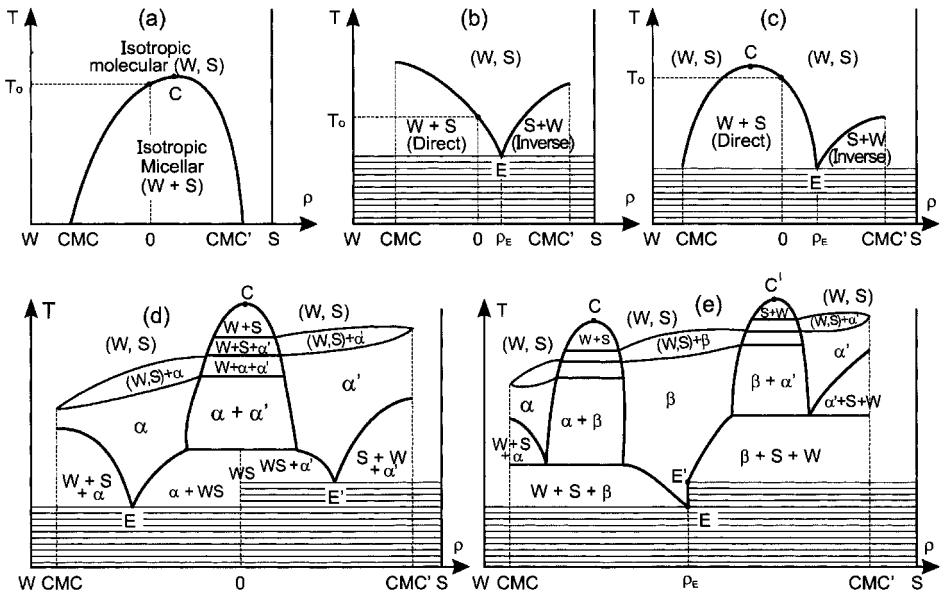

Figure 1. Working examples of temperature–concentration phase diagrams in lyotropic systems. The different figures (*a*) to (*e*) are described in the text.

the slopes of $T(\rho)$ at $\rho = \rho_E$. The univalent coefficients $a_4 < 0$ and $a_5 > 0$ are fixed by the slopes of $T(\rho)$ at $\rho = \rho_{CMC}$ and $\rho = \rho_{CMC'}$.

For the description of liquid crystalline (anisotropic) lyotropic phases, one needs to take into account symmetry-breaking order parameter(s). Assuming a single component order parameter η associated with a transition from the isotropic molecular or micellar mixture to a homogeneous liquid crystalline lyotropic phase, denoted α, the general form of the corresponding Landau expansion, truncated at the degree P' is:

$$F_L(\eta, T) = \frac{(T - T_c)}{2}\eta^2 + \sum_{m=3}^{P'} \frac{\alpha_m}{m}\eta^m \qquad (5)$$

where T_c is a critical temperature and the α_m are constant phenomenological coefficients. Therefore the total free energy which includes the ρ and η variational parameters can be written as:

$$\Phi(\Delta\mu, T) = -\Delta\mu\rho + F_G(\rho, T) + F_L(\eta, T) + F_{GL}(\rho, \eta) \qquad (6)$$

and

$$F_{GL}(\rho, \eta) = \delta_{12}\rho\eta^2 + \delta_{22}\rho^2\eta^2 + \ldots + \delta_{nm}\rho^n\eta^m \qquad (7)$$

is the coupling free-energy, the δ_{ij} being constant coupling coefficients.

Let us illustrate the procedure which allows construction of the phase diagram associated with a given free energy by considering the working example with

$$\Phi(\Delta\mu, T) = -\Delta\mu\rho + \frac{(T - T_o)}{2}\rho^2 + \frac{a_4}{4}\rho^4 + \frac{(T - T_c)}{2}\eta^2 + \frac{\alpha_4}{4}\eta^4 + \delta_{12}\rho\eta^2 \qquad (8)$$

in which the cubic ρ-invariant $\alpha_3/3\,\rho^3$ has been eliminated by redefining the zero of ρ and the coefficients $\Delta\mu$, $(T - T_o)$ and a_4 [9]. Minimizing the sum $F(\rho, \eta, T) = F_G(\rho, T) = F_L(\eta, T) + F_{GL}(\rho, \eta)$ with respect to η, at given ρ, one gets the equation of state:

$$\eta_e(T - T_c + a_4\eta_e^2 + 2\delta_{12}\rho) = 0 \qquad (9)$$

and the stability condition:

$$T - T_c + 2\delta_{12}\rho + 3\alpha_4\eta_e^2 \geqslant 0 \qquad (10)$$

where η_e denotes the equilibrium value of η. Equations (9) and (10) show that for $T \geqslant T_c - 2\delta_{12}\rho = T_1(\rho)$, one has $\eta_e = 0$ and:

$$F(\rho, \eta_e, T) = \frac{T - T_o}{2}\rho^2 + \frac{a_4}{4}\rho^4 \qquad (11)$$

whereas for $T < T_1(\rho)$ one obtains: $\eta_e = \pm[(T_1(\rho) - T)/\alpha_4]^{1/2}$ and:

$$F(\rho_1\eta_e, T) = -\frac{(T - T_c)^2}{4\alpha_4} - \frac{\delta_{12}(T - T_c)}{\alpha_4}\rho + \frac{(T - T'_o)}{2}\rho^2 + \frac{a_4}{4}\rho^4 \qquad (12)$$

with $T'_o = T_o + 2\delta_{12}^2/\alpha_4$. The common tangent construction may then be applied to the minimized functions defined by equations (11) and (12), i.e. by solving equations (1) and (2) for the two phases which are stable above and below the critical line $T = T_1(\rho)$. Figure 1 (*d*) shows the resulting phase diagram, for which the conditions $\delta_{12} > 0$, and $T_c < T_o$ have been assumed. The phase diagram is divided into two regions of similar topologies located on the right and left hand sides of the line of equal concentrations $\rho(T) = 0$. Above $T = T_1(\rho)$, where equation (11) holds, two isotropic molecular phases are separated by the isotropic micellar phase; this is bounded by an equilibrium line, the maximum of which coincides with the point of equal concentration $\rho_c(T_o) = 0$. The α and α' phases are direct and reversed ordered lyotropic phases, with the same macroscopic symmetry, determined by the symmetry of the order parameter η. Their lowest limits in temperature coincide with the eutectic points E and E′, at which merge the equilibrium lines bounding a direct micellar W + S + α (or reversed micellar S + W + α') region of coexistence and a region of coexistence of the α (or α') phase, with a phase denoted WS. In this phase, which is stabilized for $\rho(T) = 0$ (and can therefore be observed only in the demixing regions of coexistence with the α and α' phases), one has an equal amount of direct and reversed micelles.

More complex phase diagrams can be obtained by the same procedure considering higher degree expansions in ρ and η, or higher degree couplings. Figure 1 (*e*) represents the phase diagram associated with the total free energy:

$$\Phi(\Delta\mu, T) = -\Delta\mu\rho + \frac{(T - T_o)}{2}\rho^2 + \frac{a_3}{3}\rho^3 + \frac{a_4}{4}\rho^4 + \frac{a_6}{6}\rho^6 + \frac{(T - T_c)}{2}\eta^2 + \frac{\alpha_4}{4}\eta^4 + \delta_{12}\rho\eta^2 + \delta_{22}\rho^2\eta^2. \qquad (13)$$

It contains three ordered lyotropic phases (α, α' and β) having the same geometry. The α phase may represent, for example, a lamellar phase with thin W layers and thick amphiphilic layers. The α' phase has the inverted geometry, and the β phase may present a smectic-type layer periodicity requiring equivalent amounts of W and S. The phases are separated from the molecular solution

by cigar-shaped regions of coexistence, and bounded at low temperature either by regions of coexistence of micellar solutions with the β phase, or by eutectic points (E and E′).

3. Real mixtures

The procedure for construction of the phase diagrams presented above allows a systematic description of the phase diagram topologies found in real lyotropic mixtures. We shall illustrate this point by discussing two specific examples of phase diagrams found in lyotropics. We first consider the phase diagram exhibited by the sodium laurate–water system [11, 12], which is shown in figure 2(*a*). It has an almost double eutectic shape with three anisotropic lyotropic phases (lamellar L_α, intermediate rectangular R_α, and hexagonal H_α) separated from the isotropic micellar solution by biphasic regions of coexistence.

The phenomenological description of the phase diagram of figure 2(*a*) can be made as follows. Firstly, the equilibrium $T(\rho)$ curve, separating the isotropic micellar region from the ordered lyotropic phases, displays two maxima with an intermediate eutectic-type minimum. A power expansion of $T(\rho)$ should therefore be at least of the third degree in $(\rho - \rho_E)$, and $F_G(\rho - \rho_E, T)$ has to be at least of the fifth degree in $(\rho - \rho_E)$:

$$F_G(\rho-\rho_E,T)=\frac{(T-T_E)}{2}(\rho-\rho_E)^2+\frac{a_3}{3}(\rho-\rho_E)^3+\frac{a_4}{4}(\rho-\rho_E)^4+\frac{a_5}{5}(\rho-\rho_E)^5. \quad (14)$$

Simple analytical considerations deduced from the common tangent construction method, then show that $(\partial T/\partial\rho)_{\rho=\rho_E}=-a_3$, i.e. a_3 is a divalent coefficient, the values of which are determined by the slopes of $T(\rho)$ on the right and left hand sides of $\rho=\rho_E$. The effective values of a_4 and a_5 are given by the values of the tangent to the $T(\rho)$ curve at $\rho=\rho_{min}$ and $\rho=\rho_{max}$. The critical points C and C′ correspond to the concentrations $\rho_{c,c'}=-a_4/3a_5\pm(a_4^2/9a_5-a_3/3a_5)^{1/2}$.

A second step consists in determining the symmetry-breaking order parameters which describe the transitions from the isotropic micellar solution to the L_α, H_α and R_α phases. For that purpose, one has to take the following into consideration [13]. (i) The isotropic (O(3))–lamellar ($D_{\infty h}$) transition is depicted by one pair of wave-vectors $\mathbf{k}_\pm$, with $|\mathbf{k}_\pm|=\pi/d$, where d is the

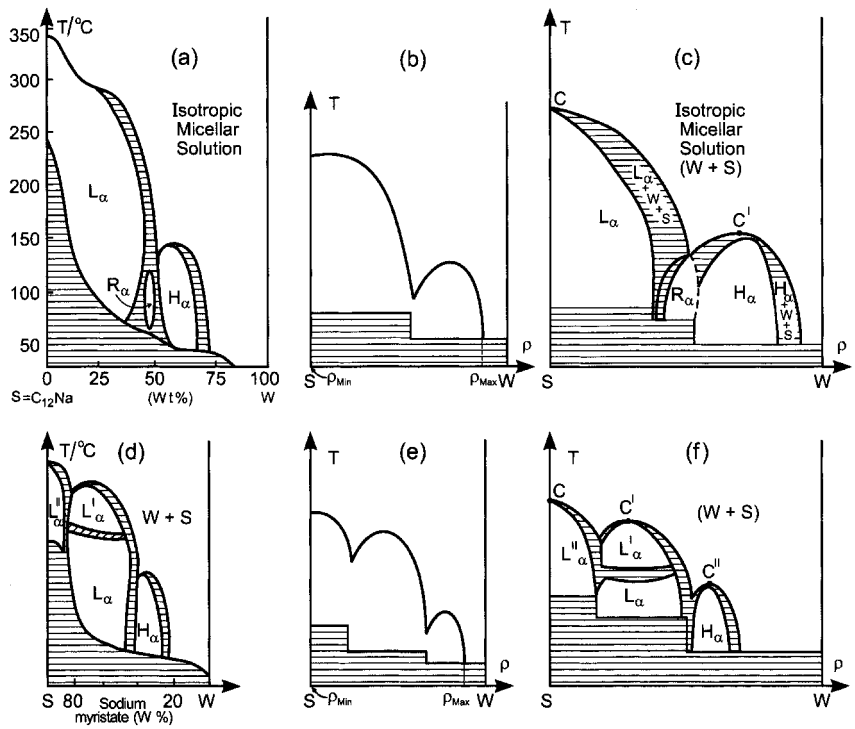

Figure 2. Illustrative examples of experimental temperature–concentration phase diagrams in lyotropic systems. The different figures (*a*) to (*f*) are described in the text.

period along the normal to the lamellae. The two non-vanishing components of the corresponding infinite-dimensional order parameter fulfil the equilibrium condition $\eta_{k+} = \eta_{k-} = \eta$, which yields the effective free-energy:

$$F^{L\alpha}(\eta, T) = \frac{(T - T_c)}{2}\eta^2 + \frac{\alpha_3}{3}\eta^3 + \frac{\alpha_4}{4}\eta^4. \qquad (15)$$

(ii) The two dimensional cylindrical mesophases H_α and R_α require two pairs of wave-vectors [13] $\pm\mathbf{k}_1$ and $\pm\mathbf{k}_2$ with $|\mathbf{k}_1| = |\mathbf{k}_2|$. One gets hexagonal (*P6m*) or *C*-centred rectangular (*Cmm*) two-dimensional space groups for, respectively, an angle γ between $\mathbf{k}_1$ and $\mathbf{k}_2$ of 120° or 90°. In both cases the four non-vanishing components of the order parameters associated with the isotropic-to-H_α and isotropic-to-R_α transitions fulfil the equilibrium conditions $\zeta_1 = \zeta_2 = \zeta_3 = \zeta_4 = \zeta$ for the H_α phase (and $\zeta'_1 = \zeta'_2 = \zeta'_3 = \zeta'_4 = \zeta'$ for the R_α phase). The corresponding effective free energies $F^{H}{}_a(\zeta, T)$ and $F^{R}{}_a(\zeta', T)$ have the same form given by equation (15), η being substituted by ζ (or ζ') and T_c by T'_c (or T''_c). Accordingly, the total effective free energy to which the phase diagram of figure 2(*a*) is associated is:

$$\begin{aligned}\Phi(\Delta\mu, T_1) = &-\Delta\mu\rho + F_G(\rho, T) + F^{L}{}_a(\eta, T) + F^{H}{}_a(\zeta, T)\\ &+ F^{R}{}_a(\zeta', T) + \rho[\delta_1\eta^2 + \delta_2\zeta^2 + \delta_3\zeta'^2]\\ &+ \mu_1\eta^2\zeta^2 + \mu_2\eta^2\zeta'^2 + \mu_3\zeta^2\zeta'^2. \qquad (16)\end{aligned}$$

The theoretical phase diagrams associated with the preceding free energy, which reflect most closely the experimental phase diagram of figure 2(*a*) are shown in figures 2(*b*) and 2(*c*). The two phase diagrams possess the same features except: (a) the transition between the H_α and R_α phases is found theoretically to be possibly second order; (b) the shape of the 'curd' region has to be fitted by assuming a smooth dependence on temperature for some of the phenomenological coefficients.

As a second example let us consider the experimental phase diagram found in the sodium myristate–water system [14] (or with a very similar topology in many alkali soap–water systems [15]) and shown in figure 2(*d*). It has a marked bieutectic shape that requires at least a sixth degree expansion of $F_G(\rho, T)$, figure 2(*c*), and differs from the phase diagram of figure 2(*a*) in two respects. First, by the absence of the intermediate R_α phase. Second, by the fact that the lamellar region is subdivided into three distinct phases (L_α, L'_α, L''_α). Hence, the same Landau expansion $F^{L}{}_a(\eta, T)$ given by equation (15) can be used for the three phases, but it has to be expanded up to the eighth degree in η, in order to account for the isostructural L'_α–L_α transition, figure 2(*f*).

4. Summary

A phenomenological approach to the temperature–concentration phase diagrams of lyotropic liquid crystals has been described, and shown to apply to experimental examples of lyotropic systems. It is based on the coupling of two types of variational parameters and free energies. First, a concentration variational parameter ρ whose corresponding free energy $F_G(\rho, T)$ is a power expansion of ρ. $F_G(\rho, T)$ accounts for the transitions between isotropic phases, as well as for the equilibrium $T(\rho)$ curve bounding the liquid crystalline region. Secondly, symmetry-breaking order parameter(s) corresponding to standard (Landau) free energies which depict the transition(s) form the isotropic micellar phase to the anisotropic liquid crystalline lyotropic phases. Increasing the number of surfactants or (and) solvents does not modify in an essential manner the method described here but increases the number of equations to be solved simultaneously.

The Fundação de Amparo à Pesquisa do Estado de São Paulo supported this work.

References

[1] Ekwall, P., 1975, in *Advances in Liquid Crystals*, Vol. 1, edited by G. H. Brown (New York: Academic Press), p. 1.
[2] Holmes, M. C., and Leaver, M. S., 1998, in *Phase Transitions in Complex Fluids*, edited by P. Tolédano and A. M. Figueiredo Neto (Singapore: World Scientific), p. 29.
[3] Yu, L. J., and Saupe, A., 1980, *Phys. Rev. Lett.*, **45,** 1000.
[4] Charvolin, J., and Sadoc, J.-F., 1994, in *Micelles, Membranes, Microemulsions and Monolayers*, edited by W. H. Gelbart, A. Ben Shaul and D. Roux (Berlin: Springer).
[5] Gompper, G., and Schick, M., 1994, in *Phase Transitions and Critical Phenomena*, Vol. 16, edited by C. Domb and J. L. Lebowitz (New York: Academic Press).
[6] Huse, D. A., and Leibler, S., 1988, *J. Phys. (Fr)*, **49,** 605.
[7] Mettout, B., Tolèdano, P., Vasseur, H., and Figueiredo Neto, A. M., 1997, *Phys. Rev. Lett.*, **78,** 3843.
[8] Tolèdano, P., and Dmitriev, V., 1996, *Reconstructive Phase Transitions* (Singapore: World Scientific).
[9] Blume, M., Emery, V. J., and Griffiths, R. B., 1971, *Phys. Rev. A*, **4,** 1071.
[10] Gibbs, J. W., 1961, in *The Scientific Papers of J. Willard Gibbs* (New York: Dover), p. 43.
[11] Husson, F., Mustacchi, M., and Luzzati, V., 1960, *Acta Cryst.*, **13,** 668.
[12] Madelmont, C., and Perron, R., 1976, *Colloid Polym. Sci.*, **254,** 581.
[13] Dmitriev, V. P., Tolèdano, P., and Figueiredo Neto, A. M., 1999, *Phys. Rev. E*, **59,** 771.
[14] Vold, R. D., Reivere, R., and McBain, I. W., 1941, *J. Am. chem. Soc.*, **63,** 1293.
[15] McBain, J. W., and Sierichs, W. C., 1948, *J. Am. oil chem. Soc.*, **25,** 221.